Online Research @ Cardiff

This is an Open Access document downloaded from ORCA, Cardiff University's institutional repository: https://orca.cardiff.ac.uk/id/eprint/108234/

This is the author's version of a work that was submitted to / accepted for publication.

Citation for final published version:

Zhu, Hanxing ORCID: https://orcid.org/0000-0002-3209-6831, Fan, Tongxiang, Peng, Qing and Zhang, Di 2018. Giant thermal expansion in 2D and 3D cellular materials. Advanced Materials 30 (18) , 1705048. 10.1002/adma.201705048 file

Publishers page: https://doi.org/10.1002/adma.201705048 <https://doi.org/10.1002/adma.201705048>

Please note:
Changes made as a result of publishing processes such as copy-editing, formatting and page numbers may not be reflected in this version. For the definitive version of this publication, please refer to the published source. You are advised to consult the publisher's version if you wish to cite this paper.

This version is being made available in accordance with publisher policies. See http://orca.cf.ac.uk/policies.html for usage policies. Copyright and moral rights for publications made available in ORCA are retained by the copyright holders.

information services
gwasanaethau gwybodaeth

ADVANCED MATERIALS

DOI: 10.1002/adma.201705048

Article type: Communication

Giant Thermal Expansion in 2D and 3D Cellular Materials

By *Hanxing Zhu* [a,*], *Tongxiang Fan* [b], *Qing Peng* [c, d] *and Di Zhang* [b]

[a] School of Engineering, Cardiff University, Cardiff, CF24 3AA, UK

[b] State Key Lab of Metal Matrix Composites, Shanghai Jiaotong University, Shanghai, 200240, China

[c] School of Power and Mechanical Engineering, Wuhan University, Wuhan 430072, China.

[d] Nuclear Engineering and Radiological Sciences, University of Michigan, Ann Arbor, Michigan 48109, United States

* Corresponding author: H.X.Z. (zhuh3@cf.ac.uk)

When temperature increases, the volume of an object changes. This property was quantified as the coefficient of thermal expansion only a few hundred years ago. Part of the reason is that the change of volume due to the variation of temperature is in general extremely small and imperceptible. Here we report abnormal giant linear thermal expansions in different types of two-ingredient micro-structured hierarchical and self-similar cellular materials. The cellular materials can be two-dimensional or three-dimensional, and isotropic or anisotropic, with a positive or negative thermal expansion due to the convex or/and concave shape in their representative volume elements respectively. The magnitude of the thermal expansion coefficient could be several times larger than the highest value reported in the literature. This study suggests an innovative approach to develop temperature-sensitive functional materials and devices.

Most materials have a positive thermal expansion coefficient (PTEC) and they expand isotropically when heated. The thermal expansion coefficient (TEC) of solid materials is usually in the order of $3\times10^{-6}\ K^{-1}$ for ceramics, $10^{-5}\ K^{-1}$ for metals, and $10^{-4}\ K^{-1}$ for polymers[1, 2]. Very few unusual materials[3-7] have a negative thermal expansion coefficient (NTEC) and their lattice dimensions shrink with heating. Large negative thermal expansion is usually anisotropic[4-6], or even shrinking in one direction and expanding in another direction. Although quite a large isotropic NTEC $\alpha=-1.2\times10^{-3}\ K^{-1}$ has been found for a solid polyacrylamide film[7], the magnitude of isotropic thermal expansion coefficient of solid materials without pores is usually very limited[3, 8].

Many researchers[9-14] aim to find materials with a negative thermal expansion coefficient because such materials are of great research interest and have important applications, e.g. activators or sensors, due to the coupled thermal-mechanical behaviour[15]. It has been recognized that the thermal expansion coefficients of one-phase or two-phase solid materials that do not contain a pore phase are always very limited in magnitude, and that three-phase materials[2, 16-18] containing a pore phase could have a much larger thermal expansion coefficient than the one-phase or two-phase solid materials. Thus, people have designed some cellular materials with an improved magnitude of NTEC[19-22]. Here we study different new types of micro-structured two-ingredient hierarchical and self-similar 2D and 3D cellular materials that can be not only isotropic (note that 'isotropic' means $\alpha_x=\alpha_y$ for 2D cellular materials and $\alpha_x=\alpha_y=\alpha_z$ for 3D cellular materials) or anisotropic, but also have either a negative or a positive linear thermal expansion coefficient with a magnitude significantly larger than any reported value in the literature.

To enhance the magnitudes of thermal expansion coefficients, the 2D and 3D cellular materials in this paper are made of two different solid ingredients A and B (Figures 1 and 2). It is assumed that ingredient A is a ceramic with a Young's modulus of $E_A = 2\times10^{11}\ \ N/m^2$ and a thermal expansion coefficient of $\alpha_A = 3\times10^{-6}\ \ K^{-1}$, and ingredient B is a polymer with a Young's modulus of $E_B = 3\times10^{9}\ \ N/m^2$ and a thermal expansion coefficient of $\alpha_B = 200\times10^{-6}\ \ K^{-1}$. Figures 1c, 1d and 1e show the geometrical structures of the periodic representative volume elements (RVEs) of the first level two-ingredient 2D cellular materials with isotropic NTEC, isotropic PTEC and anisotropic TEC, respectively. The two straight and inclined struts are made of ingredient A, perpendicular to each other, and have rigid connection in the middle. All the other struts in the RVEs of the first level (i.e. level-1) 2D cellular materials are made of ingredient B. Figure 2 shows the geometrical structures of the periodic representative volume elements (RVEs) of the first level two-ingredient 3D cellular materials with isotropic NTEC, isotropic PTEC and anisotropic TEC, respectively. The four straight and inclined struts are made of ingredient A and have rigid connection in the middle. All the other struts in the RVEs of the first level 3D cellular materials are made of ingredient B. When the effect of thermal expansion is absent, the shape of all the non-straight struts in the RVEs of both the first level 2D and 3D materials is assumed to be a chevron with a span of $L = 1.0$ and an amplitude of a, as shown in Figure 3a. Moreover, all the dimensions in Figures 1-3, including the *x, y* and *z* axes, are normalized by L. In addition, all the chevron struts are assumed to have a uniform thickness t for 2D cellular materials or a uniform square cross-section of side t for 3D cellular materials. The chevron struts (Made of ingredient B) are assumed to be pin-connected with the straight struts of the cross (made of ingredient A) in the middle.

When there is a temperature change ΔT, the change of the amplitude Δa of the chevron struts can be obtained from Equations (S1-3) and (S1-4) (see the Supporting Information), and the magnitude of the isotropic negative (Figures 1c and 2a), or isotropic positive (Figures 1d and 2b), or anisotropic (Figures 1e and 2c) linear thermal expansion coefficients of both the first level 2D and 3D cellular materials can be obtained as $\alpha_1 \approx k_1 \Delta\alpha$, where $\Delta\alpha = \alpha_B - \alpha_A \approx \alpha_B = 2\times10^{-4}\ K^{-1}$, and the linear thermal expansion magnification factor k_1 is defined as $k_1 = \alpha_1 / \Delta\alpha$ and given as

$$k_1 = \frac{1.667\Delta a}{\Delta\alpha\Delta T} \tag{1}$$

for the first level 2D cellular materials, and

$$k_1 = \frac{2.205\Delta a}{\Delta\alpha\Delta T} \tag{2}$$

for the first level 3D cellular materials. In Equations (1) and (2), $\Delta\alpha\Delta T$ is the thermal strain of the chevron struts relative to the cross in the middle. The detailed derivation of Δa, α_1 and k_1 is given in the Supporting Information (S1.1).

Figure 4a shows the effects of the dimensionless amplitude a/L and the aspect ratio t/L on the magnification factor k_1 of the positive or negative, isotropic or anisotropic linear thermal expansion coefficients of the first level 2D cellular materials with chevron struts which are pin-connected to the cross in the middle. It is noted that the values of k_1 in Figure 4a obtained from Equations (1), (2), (S1-3) and (S1-4) remain almost the same when $0.005 \le \Delta T \le 100\ K$. The results presented in Figure 4a are obtained from the small deformation theory and a single Timoshenko beam element, and the combined effects of thermal expansion, strut bending, transverse shearing and axial compression on the deformation

of the chevron struts have all been considered. We also found that the transverse shear deformation of the chevron struts has negligible effect on the values of k_1.

When a/L is 0.005 and $t/L = 0.01$, the magnification factor k_1 of the first level 2D cellular materials can have a value of 41.75. Thus, the magnitude of the linear isotropic or anisotropic NTEC or PTEC of the first level 2D cellular materials can reach $\alpha_1 = k_1 \Delta\alpha = 41.75 \times 2 \times 10^{-4} = 8.35 \times 10^{-3}\ K^{-1}$. This magnitude is much larger than the values of thermal expansion coefficient reported in references[3-8]. Moreover, if ingredient B is chosen as a polyacrylamide whose thermal expansion coefficient is $\alpha_B = -1.2 \times 10^{-3}\ K^{-1}$ (see reference[7]), the magnitude of the linear isotropic or anisotropic NTEC or PTEC of the first level 2D cellular materials could reach $|\alpha_1| = |k_1 \Delta\alpha| = 41.75 \times 1.2 \times 10^{-3} = 5.01 \times 10^{-2}\ K^{-1}$, suggesting that the giant thermal expansion could be further enhanced by a larger thermal expansion coefficient of ingredient B. With the increase of t/L, the value of k_1 reduces very quickly because the ratio of the axial compressive strain ε to the relative thermal strain $\Delta\alpha\Delta T$ increases rapidly with t/L. When a/L is 0.05 and $t/l \le 0.025$, the thermal expansion magnification factor k_1 of the first level 2D cellular materials can achieve a value of 7.943 and thus the effective linear thermal expansion coefficient can be $\alpha_1 = k_1 \Delta\alpha \ge 7.943 \times 2 \times 10^{-4} = 1.5886 \times 10^{-3}\ K^{-1}$ over the range of $0 \le \Delta T \le 5\ K$.

It is worth mentioning that the derivation of the results in Figure 4a is independent of the Young's modulus of ingredient B if the deformation of the chevron struts is linear elastic, and that the axial compression of the chevron struts can significantly reduce the value of k_1. For different types of the first level 3D cellular materials shown in Figure 2, the linear thermal expansion magnification factors of the isotropic or anisotropic NTEC or PTEC are 1.322 times those of their first level 2D cellular counterparts. It is also noted that the thermal deformation

of the chevron struts is in general a geometrical nonlinearity problem. To validate the accuracy and applicability of the results in Figure 4a, we have performed finite deformation geometrical nonlinearity analysis (see Supporting Information S1.2). The values of k_1 obtained from the geometrical nonlinearity analysis are almost the same as those presented in Figure 4a. This is partly because even when $\Delta\alpha\Delta T = 2\times10^{-3}$ (i.e, $\Delta\alpha = 2\times10^{-4}\ K^{-1}$ and $\Delta T = 10\ K$), the strain in the solid chevron struts is still smaller than 0.2%. Moreover, we have also performed finite element simulation to validate the theoretical results using the commercial finite element software ABAQUS. Half a chevron strut is partitioned into 800 plane stress CPS4T elements and the obtained results are shown in Tables S1 and S2 (in the Supporting Information) to validate the theoretical results presented in Figures 4a and 4b. For the cases when the chevron struts are pin-jointed with the cross, the FEM results in Table S1 show quite good agreement with the theoretical results presented in Figure 4a although the FEM results indicate that the larger the value of $\Delta\alpha\Delta T$, the smaller the magnification factor k_1. For the cases when the chevron struts are replaced by two pin-jointed struts (as shown in Fig. 3b), the FEM results in Table S2 are identical to the theoretical results presented in Figure 4b. When the chevron struts are rigidly connected instead of pin-jointed to the cross in the middle of the 2D or 3D cellular materials, the values of a/L remain unchanged, the thermal expansion magnification factors presented in Figure 4a are still valid when the value of $2t/L$ (instead of t/L) are used to find the corresponding k_1.

Now, if the chevron strut in Figure 3a is replaced by two pin-jointed struts as shown in Figure 3b, the values of the thermal expansion magnification factor k_1 of the first level 2D cellular materials are obtained (see S1.3) and presented in Figure 4b. For the first level 2D cellular materials when a/L is 0.001, the thermal expansion magnification factor k_1 is 375 and the linear CTE is $\alpha_1 = k_1\Delta\alpha = 375\times2\times10^{-4} = 0.075\ K^{-1}$ if $\Delta T \le 0.005\ K$; and k_1 becomes

102.3 and $\alpha_1 = k_1 \Delta\alpha = 102.3 \times 2 \times 10^{-4} = 0.0204\ K^{-1}$ if $\Delta T \le 0.5\ K$. These magnitudes are much larger than any reported thermal expansion coefficients in literature, including the results in references[2, 20], which is the highest value reported to the best of our knowledge. It is worth pointing out that the magnification factors of pin-jointed struts (Figure 4b) are sensitive to the dimensionless amplitude a/L and the temperature change ΔT. On the other side, they are entirely independent of the aspect ratio t/L. When a/L is 0.001 and $t/L \ge 0.05$, the single level 2D cellular materials still have a reasonable stiffness $E_1 \approx 1.2 \times 10^3\ N/m^2$ from Equation (S2-5). However, if a/L is too small, the 2D cellular materials with pin-jointed struts may not have a sufficient stiffness to support their self-weight and to enable the expected thermal expansion function. In general, the larger the range of the relative thermal strain $\Delta\alpha\Delta T$ (or temperature change ΔT), the smaller is the thermal expansion magnification factor k_1. The values of k_1 of the first level 3D cellular materials shown in Figure 2 are 1.322 times those of their first level 2D counterparts. Figure 4b shows that when $a/L = 0.02$ and $\Delta T \le 0.5\ K$, k_1 is always larger than 20 for the first level 2D cellular materials and larger than 26.44 for first level 3D cellular materials. The upbound value of k_1 depends on the specific stiffness, namely stiffness-to-weigth ratio, of the cellular structures. In other words, the giant thermal expansion of our proposed cellular material could be further improved by using materials with higher specific stiffness and CTE as component B.

Structural hierarchy can not only enhance the mechanical properties of materials[23-27], but may also enhance the magnitude of the linear thermal expansion coefficient of 2D and 3D cellular materials. Both the two-ingredient 2D and 3D hierarchical materials are thus assumed to be self-similar, as demonstrated in Figure 1. To enable the expected thermal expansion function, the minimum mechanical stiffness of the cellular materials is assumed to be about $E_n \approx 1.0 \times 10^3\ N/m^2$ (this is because the relative density of a hierarchical cellular material is

much lower than a normal solid material). For a two-level hierarchical 2D cellular material with pin-jointed chevron struts (as shown in Figure 3a), if $t/L = 0.045$ and a/L =0.01 (or 0.05), magnification factor of the linear thermal expansion coefficient can be obtained as $k_2 = (k_1)^2 = 6.91^2 = 47.7$ (or $7.03^2 = 49.4$) when $\Delta T \le 5$ *K*. In this case, the stiffness of the two-level hierarchical 2D cellular materials is about $E_n \approx 1.58 \times 10^3$ N/m^2. If the dimensionless amplitude $0.05 \le a/L \le 0.1$ and $0.045 \le t/L \le 0.1$, the magnification factor of the linear thermal expansion coefficient of a two-level hierarchical and self-similar 2D cellular material shown in Figure 1 can easily achieve a value of $k_2 = (k_1)^2 > 3.5^2 = 12.25$ when $\Delta T \le 5$ *K*, which is significantly greater than that of its single level counterpart with the same a/L and t/L. It is noted that for 2D or 3D cellular materials with chevron struts, the magnification factor of the linear thermal expansion coefficient strongly depends on the values of both a/L and t/L; in contrast, their mechanical stiffness is mainly dependent on the aspect ratio t/L and entirely independent of the amplitude a/L.

We have also studied the case when the chevron struts in the hierarchical and self-similar 2D and 3D cellular materials are replaced by pin-jointed struts. Figure 4b and Table S2 (in the Supporting Information) show that if $t = 0.04L = 0.04$ and $a = 0.05L = 0.05$ for a two-level hierarchical and self-similar 2D cellular material, the magnification factor of the linear thermal expansion coefficient can be obtained as $k_2 = (k_1)^2 \ge 8.375^2 = 70.14$ when $\Delta T \le 0.5$ *K*, or $k_2 = (k_1)^2 \ge 8.034^2 = 64.55$ when $\Delta T \le 5$ *K*. In this case, the mechanical stiffness of the two-level hierarchical 2D cellular materials can be obtained from Equation (S2-6) and given as $E_n = \frac{(8ta^2)^n}{(L^2+4a^2)^{3n/2}} E_B = \frac{(8\times 0.04\times 0.05^2)^2}{(1+4\times 0.05^2)^3} \times 3\times 10^9 = 1.864\times 10^3$ N/m^2. If $t = 0.1L = 0.1$ and $a = 0.06L = 0.06$, for a two-level hierarchical and self-similar 3D cellular material, the magnification factor of the linear thermal expansion coefficient can be obtained as

$k_2 = (1.322k_1)^2 \geq 1.322^2 \times 7.02^2 = 86.127$, thus $\alpha_2 = k_2 \Delta\alpha \geq 86.127 \times 2 \times 10^{-4} = 0.0172 \quad K^{-1}$ when $\Delta T \leq 0.5 \quad K$, or $k_2 = (k_1)^2 \geq 1.322^2 \times 6.815^2 = 81.17$ and $\alpha_2 = k_2 \Delta\alpha \geq 81.17 \times 2 \times 10^{-4} = 0.0162$ when $\Delta T \leq 5 \ K$. In this case, the strain or deformation of the two-level hierarchical and self-similar 3D cellular materials will be $\alpha_2 \Delta T = 0.0172 \times 0.5 = 0.86\%$ (or $\alpha_2 \Delta T = 0.0162 \times 5 = 8.1\%$) although the thermal strain in the struts is just 0.02% (or 0.2%). The mechanical stiffness of the two-level hierarchical and self-similar 3D cellular materials can be obtained from Equation (S2-8) and given as $E_n = \frac{(17.64t^2a^2)^n}{(L^2+4a^2)^{3n/2}} E_B = \frac{(17.64 \times 0.1^2 \times 0.06^2)^2}{(1+4\times 0.06^2)^3} \times 3 \times 10^9 = 1.16 \times 10^3 \ N/m^2$. If $t = 0.15L = 0.15$ and $a = 0.08L = 0.08$, for a three-level hierarchical and self-similar 2D cellular materials, the magnification factor of the linear thermal expansion coefficient can be obtained as $k_3 = (k_1)^3 \geq 5.241^3 = 143.96$ (i.e., $\alpha_3 = k_3 \Delta\alpha \geq 143.96 \times 2 \times 10^{-4} = 0.0288 \ K^{-1}$) when $\Delta T \leq 5 \ K$. In this case, the stiffness of the three-level hierarchical 2D cellular materials can be obtained from Equation (S2-6) and given as $E_n = \frac{(8ta^2)^n}{(L^2+4a^2)^{3n/2}} E_B = \frac{(8 \times 0.15 \times 0.08^2)^3}{(1+4\times 0.08^2)^{4.5}} \times 3 \times 10^9 = 1.21 \times 10^3 \ N/m^2$. For three-level hierarchical and self-similar 3D cellular materials, if $t = 0.2L = 0.2$ and $a = 0.1L = 0.1$, the magnification factor of the linear thermal expansion coefficients is obtained as $k_3 = (1.322k_1)^3 \geq 1.322^3 \times 4.28^3 = 181.1$ (i.e., $\alpha_3 = k_3 \Delta\alpha \geq 181.1 \times 2 \times 10^{-4} = 0.0362 \ K^{-1}$) when $\Delta T \leq 5 \ K$, and the stiffness of the three-level hierarchical and self-similar 3D cellular materials is given as $E_n = \frac{(17.64t^2a^2)^n}{(L^2+4a^2)^{3n/2}} E_B = \frac{(17.64 \times 0.2^2 \times 0.1^2)^3}{(1+4\times 0.1^2)^{4.5}} \times 3 \times 10^9 = 0.883 \times 10^3 \ N/m^2$.

Lakes[2, 20] has designed isotropic single–level 2D hexagonal honeycomb and 3D tetrakaidecahedral open cell foam with curved struts made of two different ingredients. They both could have a very large isotropic positive or negative thermal expansion coefficient given

by $\alpha_{RVE} = \frac{l}{h_1 + h_2}[\frac{1}{2\tan(\theta/2)} - \frac{1}{\theta}](\alpha_2 - \alpha_1) = \frac{l}{t}[\frac{1}{2\tan(\theta/2)} - \frac{1}{\theta}]\Delta\alpha = \frac{l}{t} f(\theta)\Delta\alpha$, where l and t are the length and thickness of the curved struts, θ is the angle of the curved struts and $\Delta\alpha$ is the difference of the thermal expansion coefficients of the two ingredients[20]. When $\theta = \pi$, the magnification factors of the cellular materials designed by Lakes[2, 20] are included in Fig. 4a for comparison. It is noted that θ should be smaller than 229.18^0 (i.e. 4 radians), otherwise the curved struts will overlap, and thus the maximum possible value of $f(\theta)$ is smaller than 0.48. If the aspect ratio $t/l = 0.01$, the maximum possible magnification factor of the NTEC or PNTEC of both the 2D and 3D cellular materials designed by Lakes[2, 20] can be obtained as $k_1 = \frac{\alpha_{RVE}}{\Delta\alpha} = \frac{l}{t} f(\theta) < 48$, thus $\alpha_1 = \alpha_{RVE} = k_1\Delta\alpha < 48 \times 2 \times 10^{-4} = 0.0096 \quad K^{-1}$, which is significantly smaller than some of our above reported results for the single-level 2D or hierarchical self-similar 2D and 3D cellular materials in this paper (as can be seen, *k* can be easily much larger than 50 in the materials designed in this paper). It is also noted that the aspect ratio t/l should be in general larger than 0.01 in the 2D and 3D cellular materials designed by Lakes[2, 20]. This is because the Young's modulus is

$$E_1 = 2.3(\frac{t}{L})^3 E_S \tag{3}$$

for hexagonal honeycombs[1, 20], and

$$E_1 = \frac{0.76\rho^2}{1 + 1.09\rho} E_S = \frac{0.1608(t/L)^4}{1 + 0.5014(t/L)^2} E_S \tag{4}$$

for tetrakaidecahedral open cell foams[20, 28]. In the cellular materials designed by Lakes[2, 20], if the two ingredients are chosen as a metal and a ceramic (with a Young's modulus $E_S = 2 \times 10^{11} \ N/m^2$), the cellular materials may be sufficiently stiff, but $\Delta\alpha$ would be in the order of $10^{-5} \ K^{-1}$ and the resultant thermal expansion coefficient would still be very small

compared to our results of the 2D or 3D cellular materials in this paper. If their two-ingredients are a ceramic and a polymer and $t/l = 0.01$, the Young's modulus of the cellular materials will be 6.9×10^3 N/m^2 for honeycombs and 4.82 N/m^2 for open-celled foams. Thus, the aspect ratio t/l can't be smaller than 0.01, otherwise the single level cellular materials designed by Lakes[2, 20] do not have a sufficient stiffness to support the self-weight and to enable the expected function of thermal expansion.

In this report, it has been demonstrated that although structural hierarchy can enhance the magnitude of the linear thermal expansion coefficient for cellular materials, it is impossible to achieve an 'unbounded' value due to the limit of a required minimum mechanical stiffness. The magnitude of the linear thermal expansion coefficient of an *n*th level hierarchical and self-similar cellular materials is obtained as $\alpha_n = \Delta\alpha\cdot(k_1)^n = (\alpha_B - \alpha_A)(k_1)^n$ for 2D and $\alpha_n = \Delta\alpha\cdot(1.322k_1)^2 = (\alpha_B - \alpha_A)\cdot(1.322k_1)^n$ for 3D if the shape of the RVE is convex, and $\alpha_n = \Delta\alpha\cdot(-k_1)^n = (\alpha_B - \alpha_A)(-k_1)^n$ for 2D and $\alpha_n = \Delta\alpha\cdot(-1.322k_1)^2 = (\alpha_B - \alpha_A)\cdot(-1.322k_1)^n$ for 3D if the shape of the RVE is concave. The magnitude of the isotropic NTEC, isotropic PTEC and anisotropic TEC of the cellular materials in this paper could achieve a value much larger than $0.012\ K^{-1}$ and significantly larger than the maximum possible value of CTE reported in literature, e.g. the maximum possible result of the 2D and 3D cellular materials designed by Lakes[2, 20]. The Young's modulus of ingredient B has no effect on the results of k_n and α_n, but strongly affects the stiffness of the cellular materials. The normal-auxeticity mechanical phase transition has recently been found in graphene, an atomic-thick two-dimensional hexagonal carbon[29]. The results in this paper could apply to multiscale metamaterials design[30] spanning from macro- down to micro and nano scales and our study opens a new avenue to developing more sensitive functional materials or devices. Although there might be some

technical challenges to manufacture the designed pin-jointed structures at the microscale, their broad applications could be foreseen.

References

[1] L. J. Gibson, M. F. Ashby, Cellular Solids, Pergamon press, Oxford, 1997.

[2] R. Lakes *J. Mater. Lett*. **1996**, 15, 475.

[3] T. A. Mary, J. S. O. Evans, T. Vogt, A.W. Sleight, *Science* **1996**, 272, 90.

[4] A. L. Goodwin, M. Calleja, M. J. Conterio, M. T. Dove, J. S. O. Evans, D. A. Keen, *Science* **2008**, 319, 794.

[5] X. G. Zheng, H. Kubozono, H. Yamada, K. Kato, Y. Ishiwata, C. N. Xu, *Nat. Nanotech.* **2008**, 3, 724.

[6] D. Das, T. Jacobs, L. J. Barbour, *Nat. Mater*. **2010**, 9, 36.

[7] X. Shen, C. Viney, E. R. Johnson, C. Wang, J. Q. Lu, *Nat. Chemistry* **2013**, 5, 1035.

[8] A. W. Sleight, *Annu. Rev. Mater. Sci*. **1998**, 8, 29.

[9] A. K. A. Pryde, K. D. Hammonds, M. T. Dover, V. Heine, J. D. Gales, M. C. Warren, *J. Phys.: Condens. Matter*. **1996**, 8, 10973.

[10] J. S. O. Evans, T. A. Mary, A. W. Sleight, *J. Solid State Chem*. **1998,** 137, 148.

[11] A. E. Phillips, A. L. Goodwin, G. J. Halder, P. D. Southon, C. J. Kepert, *Angew. Chem. Int. Ed*. **2008**, 47, 1396.

[12] M. Azuma, W. Chen, H. Seki, M. Czapski, S. Olga, K. Oka, M. Mizumaki, T. Watanuki, N. Ishimatsu, N. Kawamura, S. Ishiwata, M. G. Tucker, Y. Shimakawa, J. P. Attfield, *Nat. Commun*. **2011**, 2, 347.

[13] J. Chen, F. Wang, Q. Huang, L. Hu, X. Song, J. Deng, R. Yu, X. Xing, *Scientific Reports*

2013, 3, 2458.

[14] J. Chen, L. Hu, J. Deng, X. Xing, *Chem. Soc. Rev*. **2015**, 44, 3522.

[15] J. A. Burg, R. H. Dauskerdt, *Nat. Mater*. **2016**, 15, 974.

[16] J. Gribb, *Nature* **1968**, 220, 576.

[17] R. A. Schapery, *J. Compos. Mater*. **1968**, 2, 380.

[18] B. W. Rozen, Z. Hashin, *Int. J. Eng. Sci*. **1970**, 8, 157.

[19] O. Sigmund, S. Torquato, *Appl. Phys. Lett*. **1996**, 69, 3203.

[20] R. Lakes, *Appl. Phys. Lett*. **2007**, 90, 221905.

[21] Q. Wang, J. A. Jackson, Q. Ge, J. B. Hopkins, C. M. Spadaccini, N. X. Fang, *Phys. Rev. Lett*. **2016**, 117, 175901.

[22] L. Wu, B. Li, J. Zhou, *ACS Appl. Mater. Interfaces* **2016**, 8, 17721.

[23] R. Lakes, R. *Nature* **1993**, 361, 511.

[24] B. Ji, H. Gao, *J. Mech. Phys. Solids* **2004**, 52, 1963.

[25] H. X. Zhu, L. Yan, R. Zhang, X. M. Qiu, *Acta Mater*. **2012**, 60, 4927.

[26] H. X. Zhu, Z. B. Wang, Z.B. *Sci. Adv. Mater*. **2013**, 5, 677.

[27] X. Zheng, et al. *Science* **2014**, 344, 1373.

[28] H. X. Zhu, J. F. Knott, N. J. Mills, *J. Mech. Phys. Solids* **1997**, 45, 319.

[29] B. Deng, J. Hu, H. Zhu, S. Liu, L. Liu, Y. Shi, Q. Peng, *2D Mater*. **2017**, 4, 021020.

[30] X. Zheng, W. Smith, J. Jackson, B. Moran, H. Cui, D. Chen, J. Ye, N. Fang, N. Rogriguez, T. Weisgraber, C. M. Spadaccini, *Nat. Mater*. **2016**, 15, 1100.

Figures

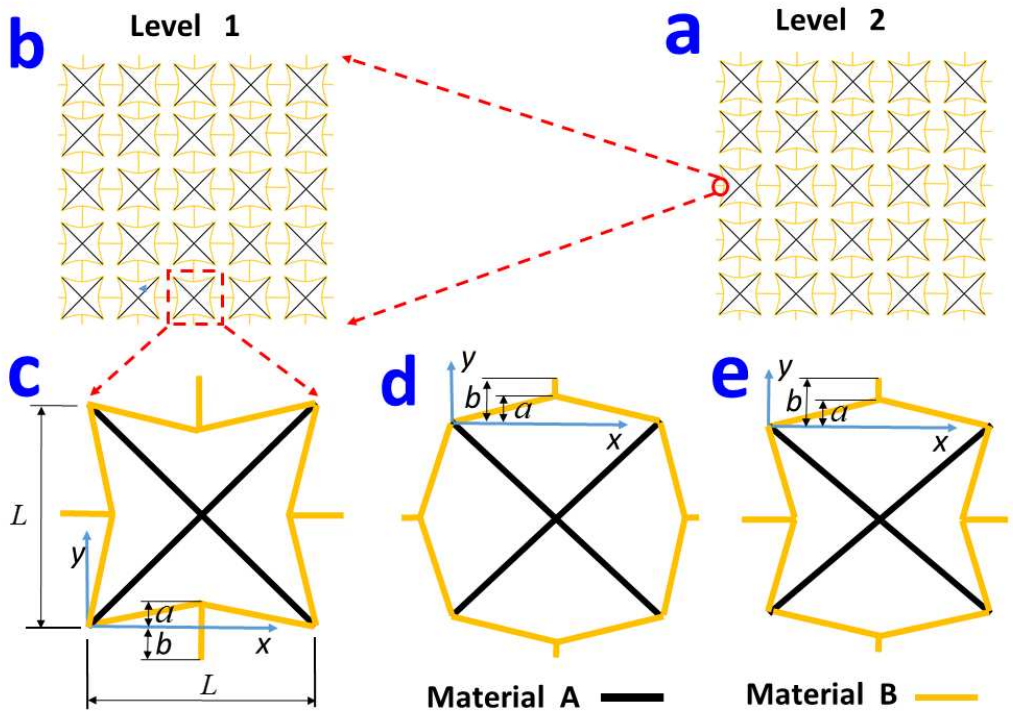

Figure 1. Geometrical structures of two-ingredient hierarchical 2D cellular materials. a) overview of the second level 2D cellular material consisting of 5×5 RVEs with non-straight struts made of the level-1 material shown in b. b) overview of the first level 2D cellular material consisting of 5×5 identical RVEs shown in c (or d or e). c) RVE of isotropic negative thermal expansion coefficient. d) REV of isotropic positive thermal expansion coefficient. e) REV of anisotropic thermal expansion coefficients.

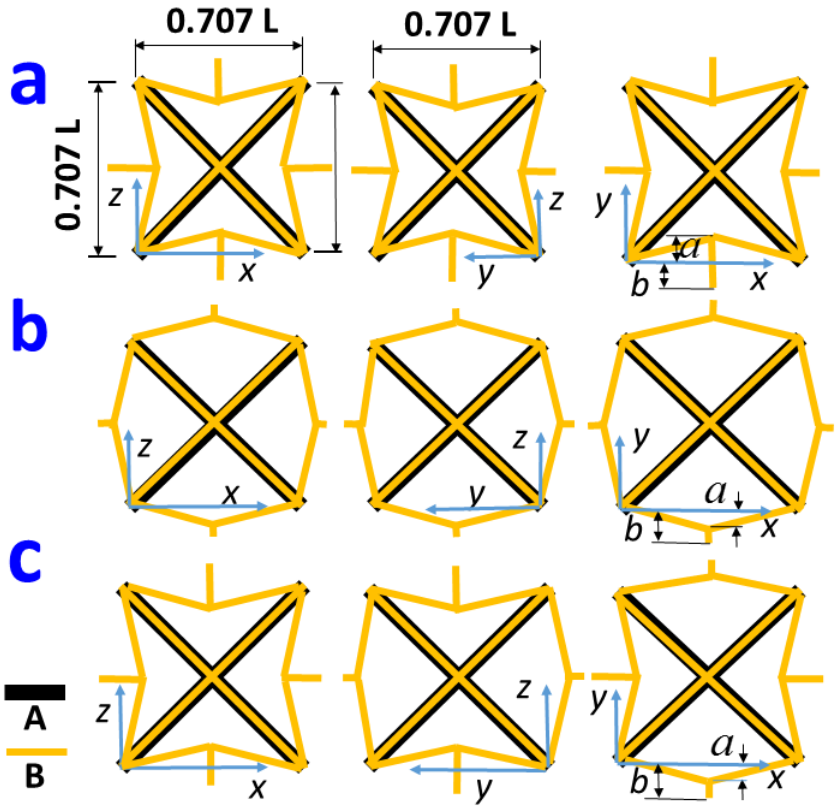

Figure 2. Geometrical structures of two-ingredient 3D cellular materials. a) RVE of isotropic negative thermal expansion coefficient. b) RVE of isotropic positive thermal expansion coefficient. c) RVE of anisotropic thermal expansion coefficients.

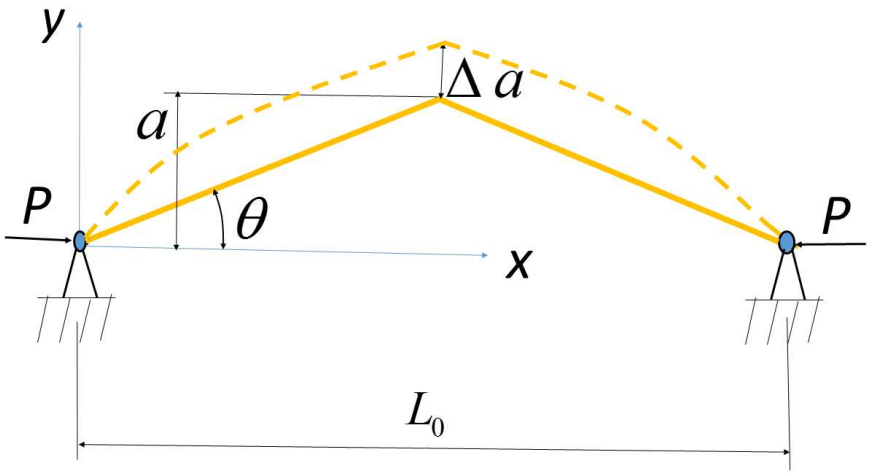

(a)

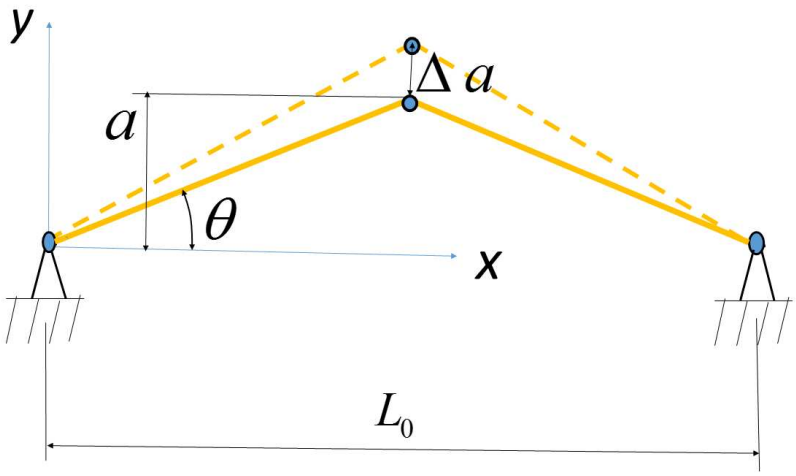

(b)

Figure 3. (a) The configuration of the chevron struts made of ingredient B before and after thermal deformation; (b) The configuration of the pin-jointed struts made of ingredient B before and after thermal deformation

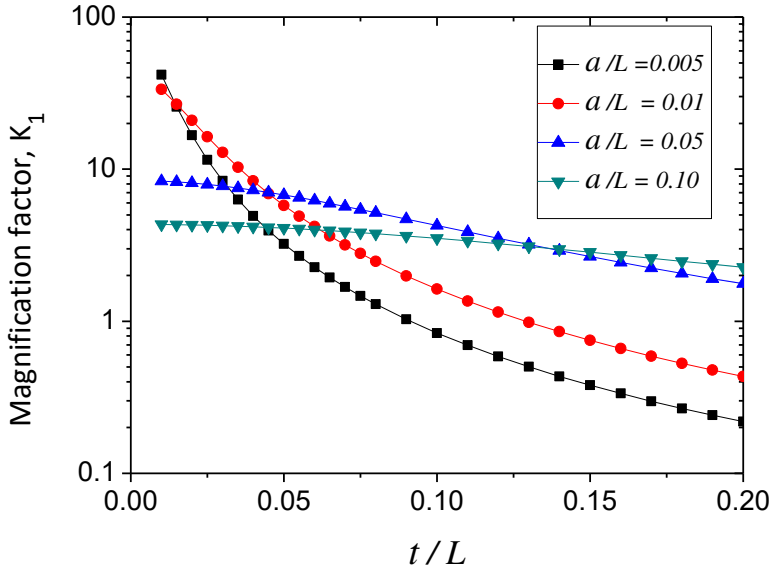

(a)

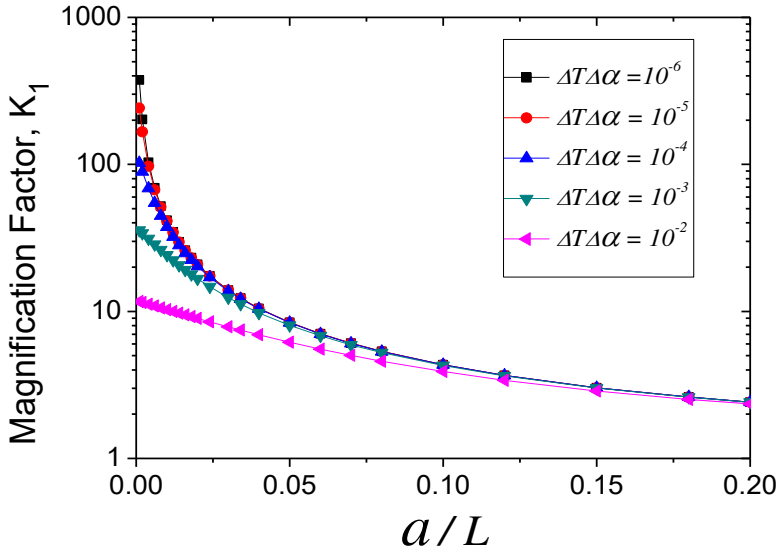

(b)

Figure 4 . Magnification factor k_1 of the positive or negative, isotropic or anisotropic linear thermal expansion coefficients of the first level 2D cellular materials: (a) with chevron struts which are pin-connected to the cross; (b) with pin-jointed struts.

ADVANCED MATERIALS

Supporting Information

DOI: 10.1002/adma.201705048

Giant Thermal Expansion in 2D and 3D Cellular Materials

By *Hanxing Zhu* [a,*], *Tongxiang Fan* [b], *Qing Peng* [c, d] *and Di Zhang* [b]

[a] School of Engineering, Cardiff University, Cardiff, CF24 3AA, UK

[b] State Key Lab of Metal Matrix Composites, Shanghai Jiaotong University, Shanghai, 200240, China

[c] School of Power and Mechanical Engineering, Wuhan University, Wuhan 430072, China.

[d] Nuclear Engineering and Radiological Sciences, University of Michigan, Ann Arbor, Michigan 48109, United States

* Corresponding author: H.X.Z. (zhuh3@cf.ac.uk)

S1. Thermal Expansion in the first level cellular materials

All types of the 2D and 3D cellular materials shown in Figures 1 and 2 are assumed to be made of two different solid ingredients A and B. Ingredient A is chosen as a ceramic with a Young's modulus of $E_A = 2\times10^{11}\ \ N/m^2$ and a thermal expansion coefficient of $\alpha_A = 3\times10^{-6}\ \ K^{-1}$, and ingredient B is chosen as a polymer with a Young's modulus of $E_B = 3\times10^{9}\ \ N/m^2$ and a thermal expansion coefficient of $\alpha_B = 200\times10^{-6}\ \ K^{-1}$. All the non-straight struts are assumed to have the same chevron shape with a span of $L = 1.0$ and an amplitude of a, and to be pin-connected with the straight struts of the cross in the middle of the RVEs. In addition, all the chevron struts are assumed to have the same uniform thickness t for 2D cellular materials or the same uniform square cross-section of side t for 3D cellular materials. Moreover, all the dimensions in Figures 1-3, including the *x, y* and *z* axes, are normalized by L. It is noted that the geometrical structure of ingredient B in Fig. 1c is similar to the 4-star auxetic honeycomb[31].

S1.1. Small linear deformation analysis of chevron struts

A temperature increase ΔT can result in a compressive force P at the two ends of the chevron struts due to the thermal mismatch between the chevron struts and the cross in the middle of the RVEs, as illustrated in Figure 3a. Small deformation analysis is based on the initial configuration of the structure, the axial compressive strain in the longitudinal direction of the chevron struts can thus be obtained as

$$\varepsilon = \frac{P\cos\theta}{E_B A} \tag{S1-1}$$

Where E_B is the Young's modulus of ingredient B and A is the cross-sectional area of the chevron struts. Obviously, the magnitude of the axial compressive strain ε can't be larger than the relative thermal strain of the chevron struts $\Delta\alpha\Delta T = (\alpha_B - \alpha_A)\Delta T$. If $\alpha_B = \alpha_A$, the thermal expansion coefficients of all different types of the first level 2D and 3D cellular materials shown in Figures 1 and 2 would be the same as α_A. It is noted that all the straight struts of the cross in the middle of the 2D and 3D RVEs undergo uniaxial tension (or compression) due to the structural symmetry. Thus, the effects of their tensile deformation on the thermal expansion are negligible because $E_A >> E_B$.

Taking account the combined effects of thermal expansion and bending, axial compression and transverse shear of the chevron struts, according to the symmetry, the following deformation compatibility condition in the longitudinal direction of half a chevron strut in Fig. 3a must be satisfied[32].

$$\frac{[\frac{L}{2\cos\theta}(1+\Delta\alpha\Delta T-\varepsilon)]^3 P\sin\theta}{3E_B I}\tan\theta + \frac{1.2\times 2(1+v_B)}{E_B A}(\frac{L}{2\cos\theta})(P\sin\theta)\tan\theta = (\Delta\alpha\Delta T-\varepsilon)\frac{L}{2\cos\theta} \tag{S1-2}$$

Where $\Delta\alpha\Delta T$ is the relative thermal strain of the chevron strut and ε given by (S1-1) is the axial compressive strain in the longitudinal direction of the chevron struts, I is the second moment of the cross-sectional area of the chevron struts, the Poisson ratio v_B of ingredient B (i.e. polymer) is taken as 0.5 and the transverse shear coefficient of the square cross-section of the chevron struts is 1.2. In Eq. (S1-2), the first and second terms on the left hand side are associated to beam bending and transverse shear deformation[32], respectively, and the term on the right hand side is the elongation of half a chevron strut in its longitudinal direction due to thermal expansion and axial compression. Substituting Eq. (S1-1) into Eq. (S1-2) leads to

$$c_1(1+\Delta\alpha\Delta T-\varepsilon)^3\varepsilon+c_2\varepsilon=\Delta\alpha\Delta T-\varepsilon \tag{S1-3}$$

Where $c_1=\frac{Aa^2(L^2+4a^2)}{3IL^2}$ and $c_2=\frac{14.4a^2}{L^2}$. Equation (S1-3) indicates that the magnitude of the axial compressive strain ε in the longitudinal direction of the chevron struts is a nonlinear function of c_1, c_2 and $\Delta\alpha\Delta T$.

For given values of c_1, c_2 and $\Delta\alpha\Delta T$, ε can be solved from Eq. (S1-3) using the Newton-Raphson method, and the change of the amplitude of the chevron struts can be obtained as

$$\Delta a=\frac{L(\Delta\alpha\Delta T-\varepsilon)}{2\sin\theta\cos\theta}=\frac{L^2+4a^2}{4a}(\Delta\alpha\Delta T-\varepsilon) \tag{S1-4}$$

For the first level 2D cellular materials with pin-connections between the chevron struts and the cross in the middle, as shown in Figure 1c, the total change of the dimensionless size of the RVE due to the combined effects of temperature change ΔT and the resultant internal force P can be obtained as

$$\Delta_{RVE}=-2\Delta a+\alpha_A\Delta T+2(a+b)\alpha_B\Delta T \tag{S1-5}$$

From the dimensionless dimensions given in Figure 1c, the isotropic negative linear thermal expansion coefficient (NTEC) of the first level 2D cellular material can be derived as

$$\alpha_1 = \alpha_{RVE} = \frac{\Delta_{RVE}}{(1+2b)\Delta T} = \frac{\alpha_A + 2(b-a)\alpha_B}{1+2b} - \frac{2\Delta a}{(1+2b)\Delta T} \approx -\frac{1.667\Delta a}{\Delta\alpha\Delta T}\Delta\alpha = -k_1\Delta\alpha \qquad \text{(S1-6)}$$

Where the dimensionless value of $b = b/L$ is chosen as 0.1, and Δa is given by Equation (S1-4). Thus $k_1 = \frac{1.667\Delta a}{\Delta\alpha\Delta T}$ is the approximate magnification factor of the NTEC. The first term in Equation (S1-6) can be neglected because its magnitude is much smaller than the second term. For given values of t/L, a/L and $\Delta\alpha\Delta T$, the magnification factor of the linear negative thermal expansion coefficient, k_1, can be obtained from Equations (S1-3), S1-4) and (S1-6).

For the first level 2D cellular materials with the geometrical structure shown in Figure 1d, the isotropic positive linear thermal expansion coefficient (PTEC) can be obtained in the similar manner and given as

$$\alpha_1 = \alpha_{RVE} = \frac{\Delta_{RVE}}{(1+2b)\Delta T} = \frac{\alpha_A + 2(b-a)\alpha_B}{1+2b} + \frac{2\Delta a}{(1+2b)\Delta T} \approx \frac{1.667\Delta a}{\Delta\alpha\Delta T}\Delta\alpha = k_1\Delta\alpha \qquad \text{(S1-7)}$$

Where the dimensionless $b = b/L$ is again chosen as 0.1. Similarly, the first level 2D cellular materials with the geometrical structure shown in Figure 1e have anisotropic linear thermal expansion coefficients of $k_1\Delta\alpha$ in one direction and $-k_1\Delta\alpha$ in the orthogonal direction.

For the first level 3D cellular materials with the geometrical structure of the representative volume element (i.e. RVE) shown in Figure 2a, the isotropic negative linear thermal expansion coefficient can be obtained as

$$\alpha_1 = \alpha_{RVE} = \frac{\Delta_{RVE}}{(1/\sqrt{2}+2b)\Delta T} = \frac{\alpha_A + 2(b-a)\alpha_B}{1/\sqrt{2}+2b} - \frac{2\Delta a}{(1/\sqrt{2}+2b)\Delta T} \approx -\frac{2.205\Delta a}{\Delta\alpha\Delta T}\Delta\alpha = -k_1\Delta\alpha \qquad \text{(S1-8)}$$

where Δa is given by Equation (S1-4).

Similarly, the isotropic positive linear thermal expansion coefficient of the first level 3D cellular materials with the geometrical structure given in Figure 2b and the anisotropic linear thermal expansion coefficient of the first level 3D cellular materials with the geometrical structure shown in Figure 2c can be derived as

$$\alpha_1 = \alpha_{RVE} = \frac{\Delta_{RVE}}{(1/\sqrt{2}+2b)\Delta T} = \frac{\alpha_A + 2(b-a)\alpha_B}{1/\sqrt{2}+2b} + \frac{2\Delta a}{(1/\sqrt{2}+2b)\Delta T} \approx \frac{2.205\Delta a}{\Delta\alpha\Delta T}\Delta\alpha = k_1\Delta\alpha \qquad \text{(S1-9)}$$

In Equations (S1-8) and (S1-9), the dimensionless dimension $b = b/L$ is also chosen as 0.1. Thus, the magnification factor of the positive, or negative, isotropic or anisotropic linear thermal expansion coefficient of the first level 3D cellular materials is $k_1 = \frac{2.205\Delta a}{\Delta\alpha\Delta T}$, which is 1.322 times that of the first level 2D cellular materials. Here, isotropic thermal expansion means that $(\alpha_{RVE})_x = (\alpha_{RVE})_y$ for 2D cellular materials and $(\alpha_{RVE})_x = (\alpha_{RVE})_y = (\alpha_{RVE})_z$ for 3D cellular materials.

Figure 4a shows the effects of the dimensionless amplitude a/L and the aspect ratio t/L of the chevron struts on the magnification factor k_1 of the positive or negative, isotropic or anisotropic linear thermal expansion coefficients of the first level 2D cellular materials with chevron struts which are pin-connected to the cross in the middle of the RVEs. It is noted that the magnitude of k_1 obtained from the above theoretical analysis is almost independent of the value of the relative thermal strain $\Delta\alpha\Delta T$ when $2\times10^{-6} \le \Delta\alpha\Delta T \le 0.02$. In addition, when a/L is smaller than 0.005, the magnitude of k_1 becomes smaller. This is because the ratio of $\varepsilon/\Delta\alpha\Delta T$ becomes larger with the reduction of a/L. We also found that the transverse shear deformation of the chevron struts has negligible effect on the magnitude of the magnification factor k_1.

Figure 4a shows that when a/L is 0.005 and $t/L = 0.01$, the magnification factor k_1 of the first level 2D cellular materials is 41.75. The magnitudes of the linear isotropic or anisotropic NTEC or PTEC of the first level 2D cellular materials can thus reach $\alpha_1 = k_1 \Delta\alpha = 41.75 \times 2 \times 10^{-4} = 8.35 \times 10^{-3}\ K^{-1}$. This value is significantly larger than the positive or negative thermal expansion coefficients reported in references[3-8]. Moreover, if the ingredient B is chosen as a polyacrylamide material whose thermal expansion coefficient is $\alpha_B = -1.2 \times 10^{-3}\ K^{-1}$ (see reference[7]), the magnitude of the linear isotropic or anisotropic NTEC or PTEC of the first level 2D cellular materials could reach $\alpha_1 = k_1 \Delta\alpha = 41.75 \times 1.2 \times 10^{-3} = 5.01 \times 10^{-2}\ K^{-1}$, suggesting that the giant thermal expansion could be further improved by the thermal expansion coefficient of ingredient B.

It is noted that the derivation of the results in Figure 4a is independent of the Young's modulus of ingredient B as long as the deformation is linear elastic, as can be seen that E_B is absent in Equations (S1-3) and (S1-4). Although the transverse shear deformation of the chevron struts has negligible effect on the magnitude of k_1, the axial compression can significantly reduce the value of k_1. If without the effect of axial compression (i.e. if ε is zero in Equation (S1-4)), the magnification factor of the linear isotropic or anisotropic NTEC or PTEC of the first level 2D cellular materials would become $k_1 = \dfrac{1.667\Delta a}{\Delta\alpha\Delta T} = 1.667(a + \dfrac{L^2}{4a})$, which is independent of the aspect ratio t/L. In this case, $k_1 = 83.35$ if $a/L = 0.005$; and $k_1 = 41.68$ if $a/L = 0.01$, being much larger than those presented in Figure 4a.

S1.2. Nonlinear finite deformation analysis of chevron struts

The analysis in S1.1 and the results shown in Figure 4a are based on the initial undeformed configuration and obtained from the small deformation theory using a single Timoshenko beam element[32]. However, the thermal deformation of the chevron struts is in general a geometrical

nonlinearity problem. The deformed configuration of half a chevron strut under thermal expansion and the restraint force P acted at the pin-jointed end is shown in Figure S1. The relationship between the bending curvature and the bending moment is given as [33, 34]

$$E_B I \frac{d\beta_b}{ds} = -Py = -\int_0^S P[(1+\Delta\alpha\Delta T - \frac{P}{E_B A}\cos\beta)\sin\beta]ds \quad \text{(S1-10)}$$

Where the left hand side is the bending stiffness times the bending curvature and the right hand side is the bending moment. When $S = l = L/(2\cos\theta)$, $\beta_b(l) = \alpha = \frac{\pi}{2} - \theta$ (see Figures 3a and S1), thus the angle $\beta_b(s)$ of the chevron strut due to the combined effects of strut bending, thermal expansion and axial compression can be determined as

$$\beta_b(s) = \frac{\pi}{2} - \theta + \frac{P}{E_B I}\int_s^l [\int_0^s (1+\Delta\alpha\Delta T - \frac{P}{E_B A}\cos\beta)\sin\beta ds]ds$$

$$= \frac{\pi}{2} - \theta + \frac{12\varepsilon_1}{t^2}\int_s^l [\int_0^s (1+\Delta\alpha\Delta T - \varepsilon_1\cos\beta)\sin\beta ds]ds \quad \text{(S1-11)}$$

In the above equation, the strut is assumed to have a square cross-section of side *t* and $\varepsilon_1 = \frac{P}{E_B A} = \varepsilon/\cos\theta$.

The angle due to transverse shear deformation of the strut is given as

$$\beta_S(s) = \frac{1.2P\sin\beta}{G_B A} = \frac{2.4(1+v)P}{E_B A}\sin\beta = 3.6\varepsilon_1\sin\beta \quad \text{(S1-12)}$$

Where the Poisson ratio of the chevron material (i.e. a polymer) is chosen as 0.5.

The total angle of the deformed half chevron strut can thus be obtained as

$$\beta(s) = \beta_b(s) + \beta_S(s) \quad \text{(S1-13)}$$

For a given value of the relative thermal strain $\Delta\alpha\Delta T$, the function $\beta(s)$ can be determined using the iterative method [33, 34] and the deformation compatibility condition:

$$\int_0^l (1+\Delta\alpha\Delta T-\varepsilon_1\cos\beta)\cos\beta ds = l\cos\theta = L/2 \tag{S1-14}$$

To solve the nonlinear function $\beta(s)$, the length of half the chevron strut $l = L/(2\cos\theta)$ was divided into 100000 elements, the value of ε_1 was initially chosen as $\Delta\alpha\Delta T/2$ and $\beta(s)$ as θ. Using the iterative method, the convergent solution of $\beta(s)$ was very quickly obtained from the following solution scheme [33, 34]. The first step is to obtain new values of $\beta(s)$ using Equations (S1-11), (S1-12) and (S1-13), and the initially given or the already obtained values of ε_1 and $\beta(s)$. The second step is to check with the deformation compatibility condition (S1-14). In step 3, if the left hand side of Eq. (S1-14) is larger than the right hand side, it suggests that the value of ε_1 is too small, then increase the value of ε_1; if the left hand side of Eq. (S1-14) is smaller than the right hand side, it suggests that the value of ε_1 is too large, then reduce the value of ε_1. Step 4 is to check the new values of $\beta(s)$ with the previous values, if the largest difference is smaller than 10^{-6}, convergent solution of $\beta(s)$ has been obtained; otherwise repeat steps 1-4 using the updated values of ε_1 and $\beta(s)$. Thus very accurate solution of $\beta(s)$ can be very quickly obtained for any given value of the relative thermal strain $\Delta\alpha\Delta T$, and the change of the amplitude of the chevron strut, Δa, can be obtained as

$$\Delta a = \int_0^l (1+\Delta\alpha\Delta T-\varepsilon_1\cos\beta)\sin\beta ds - a \tag{S1-15}$$

It is noted that in the analysis of S1.1 and S1.2, the combined effects of thermal expansion, bending, axial compression and transverse shear on the thermal deformation of the chevron

struts are all considered. The thermal expansion magnification factor of the 2D and 3D cellular materials can be obtained using the relevant equations given in section S1.1.

S1.3. Deformation analysis of pin-jointed struts

If the chevron strut in Figure 3a is replaced by two pin-jointed struts as shown in Figure 3b, for a given value of the relative thermal expansion $\Delta\alpha\Delta T$, the change of the amplitude in Figure 3b can be obtained as

$$\Delta a = \sqrt{(L^2/4 + a^2)(1+\Delta\alpha\Delta T)^2 - L^2/4} - a \tag{S1-16}$$

and the values of the thermal expansion magnification factor k_1 of the 2D cellular materials can be obtained using the relevant equations given in section S1.1, and presented in Figure 4b for 2D cellular materials. For the first level 3D cellular materials with pin-jointed struts, the values of the thermal expansion magnification factor are 1.322 times those of their 2D counterparts.

S1.4. Validation by finite element simulation

To verify the theoretical results given in Figures 4a and 4b for the first level 2D cellular materials, we have performed finite element simulation using the commercial software ABAQUS. Half a chevron strut is partitioned into 800 plane stress CPS4T elements and the obtained results are shown in Tables S1 and S2 to validate the theoretical results of Figures 4a and 4b. For the cases when the chevron struts are pin-jointed with the cross, the FEM results in Table S1 show quite good agreement with theoretical results although the FEM results indicate that the larger the value of $\Delta\alpha\Delta T$, the smaller the magnification factor k_1. For the cases when the chevron struts are replaced by two pin-jointed struts, the FEM results in Table S2 are identical to the theoretical results.

S1.5. Thermal expansion coefficient of hierarchical and self-similar cellular materials

For the *n*th level hierarchical and self-similar 2D cellular materials shown in Figure 1, the thermal expansion coefficient can be obtained as

$$\alpha_n = \Delta\alpha \cdot (k_1)^n = (\alpha_B - \alpha_A)(k_1)^n \tag{S1-17}$$

if the shape of the RVE is convex, and

$$\alpha_n = \Delta\alpha \cdot (-k_1)^n = (\alpha_B - \alpha_A)(-k_1)^n \tag{S1-18}$$

if the shape of the RVE is concave.

For the *n*th level hierarchical and self-similar 3D cellular materials, the thermal expansion coefficient can be obtained as $\alpha_n = \Delta\alpha \cdot (1.322k_1)^2 = (\alpha_B - \alpha_A) \cdot (1.322k_1)^n$ if the shape of the RVE is convex, and $\alpha_n = \Delta\alpha \cdot (-1.322k_1)^2 = (\alpha_B - \alpha_A) \cdot (-1.322k_1)^n$ if the shape of the RVE is concave.

S2. The stiffness of 2D and 3D cellular materials

When a uniaxial tensile stress σ_x is applied to the RVEs of the first level 2D cellular materials with chevron struts, as shown in Figures 1c, 1d and 1e, the concentrated force applied at the vertex of the chevron strut on the left hand side or right hand side is $F = \sigma_x(L + 2b) = 1.2L\sigma_x$, where $b = 0.1L$. The chevron struts can be treated as pin-supported beams with a span of *L* and the horizontal deformation of the RVEs can thus be approximated as $\Delta_x = \frac{2FL^3}{48E_B I} = \frac{0.6\sigma_x L^4}{E_B t^3}$ where $I = \frac{t^3}{12}$. This is because bending of the chevron struts is the dominant deformation mechanism. The horizontal strain can be derived as $\varepsilon_x = \Delta_x / (L + 2b) = \Delta_x / (1.2L) = \sigma_x L^3 / (2E_B t^3)$. Thus the Young's modulus of the first level 2D cellular materials is obtained as

$$E_1 = \frac{\sigma_x}{\varepsilon_x} = 2(\frac{t}{L})^3 E_B \quad \text{(S2-1)}$$

For the *n*th level hierarchical and self-similar 2D cellular materials, the Young's modulus can be obtained in the similar manner, and given as

$$E_n = 2(\frac{t}{L})^3 E_{n-1} = 2^n (\frac{t}{L})^{3n} E_B \quad \text{(S2-2)}$$

Similarly, the Young's modulus of the first level 3D cellular materials with pin-jointed chevron struts can be obtained as

$$E_1 = \frac{\sigma_x}{\varepsilon_x} = \frac{4t^4 E_B}{(\sqrt{2}L/2 + 2b)L^3} = 4.41(\frac{t}{L})^4 E_B \quad \text{(S2-3)}$$

For the *n*th level hierarchical and self-similar 3D cellular materials, the Young's modulus is obtained as

$$E_n = 4.41(\frac{t}{L})E_{n-1} = 4.41^n (\frac{t}{L})^{4n} E_B \quad \text{(S2-4)}$$

If the chevron strut in Figure 3a is replaced by two pin-jointed struts with a uniform thickness *t* for 2D cellular materials, as shown in Figure 3b, when a uniaxial tensile stress σ_x is applied to the RVEs of the first level 2D cellular materials, as shown in Figures 1c, 1d and 1e, the axial tensile force in each of the two pin-jointed struts is $N = \frac{\sigma_x (L+2b)}{2\sin\theta}$ and the elongation of the struts is $\Delta = \frac{NL}{2E_B t\cos\theta} = \frac{\sigma_x L(L+2b)}{4tE_B \sin\theta\cos\theta}$. Thus the tensile strain of the 2D RVE in the *x* direction is $\varepsilon_x = \frac{2\Delta}{(L+2b)\sin\theta} = \frac{\sigma_x L}{2E_B t\sin^2\theta\cos\theta}$, and the Young's modulus of the first level 2D cellular materials is obtained as

$$E_1 = \frac{\sigma_x}{\varepsilon_x} = \frac{2E_B t\sin^2\theta\cos\theta}{L} = \frac{8ta^2}{(L^2+4a^2)^{3/2}} E_B \quad \text{(S2-5)}$$

For the *n*th level hierarchical and self-similar 2D cellular materials, the Young's modulus can be obtained in the similar manner, and given as

$$E_n = \frac{8ta^2}{(L^2+4a^2)^{3/2}} E_{n-1} = \frac{(8ta^2)^n}{(L^2+4a^2)^{3n/2}} E_B \quad \text{(S2-6)}$$

Similarly, the Young's modulus of the first level 3D cellular materials is obtained as

$$E_1 = \frac{\sigma_x}{\varepsilon_x} = \frac{t^2 a^2 E_B}{(L^2/4 + a^2)^{3/2}(\sqrt{2}L/4 + b)} = \frac{17.64 t^2 a^2}{(L^2 + 4a^2)^{3/2}} E_B \quad \text{(S2-7)}$$

where $b = 0.1L = 0.1$.

For the *n*th level hierarchical and self-similar 3D cellular materials, the Young's modulus can be obtained as

$$E_n = \frac{(17.64 t^2 a^2)^n}{(L^2 + 4a^2)^{3n/2}} E_B \quad \text{(S2-8)}$$

References

[31] J.N. Grima, R. Gatt, A. Alderson, K.E. Evans, *Molecular Simulation.* **2005**, 31, 925.

[32] J.M. Gere, S.P. Timoshenko, Mechanics of Materials, Cambridge University Press, 1985.

[33] H.X. Zhu, N.J. Mills, *Int. J. Solids and Struct.* **2000**, 37, 1931.

[34] H.X. Zhu, N.J Mills, J.F. Knott, *J. Mech. Phys. Solids* **1997**, 45, 1875.

Figure

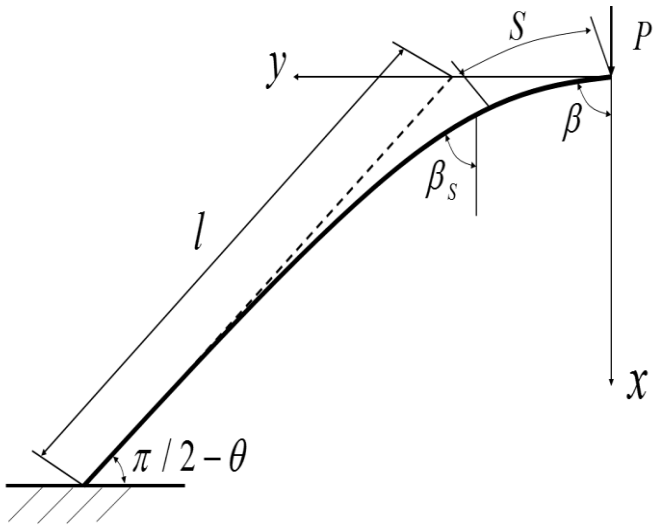

Figure S1. The deformed half chevron strut under thermal expansion and restraint force P.

Table S1. FEM validation for results presented in Figure 4a.

t/L	a/L	ΔT (K)	k_1 (theoretical result)	k_1 (FEM result)
0.01	0.005	1	41.763	40.225
0.01	0.005	1.5	41.763	37.512
0.025	0.05	5	7.943	7.578
0.025	0.05	25	7.943	6.594
0.045	0.05	0.5	7.028	6.9015
0.045	0.05	5	7.028	6.7612

Table S2. FEM validation for results presented in Figure 4b.

a/L	ΔT (K)	k_1 (Theoretical result)	k_1 (FEM result)
0.001	0.005	374.58	374.658
0.001	0.5	102.36	102.38
0.001	5	35.648	35.662
0.05	0.5	8.375	8.376
0.05	5	8.034	8.035
0.08	5	5.2431	5.243
0.1	5	4.2805	4.2806